Astronomy & Astrophysics manuscript no. output
August 17, 2022

LETTER TO THE EDITOR

A Stream Come True – Connecting tidal tails, shells, streams, and planes with galaxy kinematics and formation history

Lucas M. Valenzuela[1] and Rhea-Silvia Remus[1]

Universitäts-Sternwarte, Fakultät für Physik, Ludwig-Maximilians-Universität München, Scheinerstr. 1, 81679 München, Germany
e-mail: lval@usm.lmu.de

Received XXX / Accepted YYY

ABSTRACT

Context. The rapidly improving quality and resolution of both low surface brightness observations and cosmological simulations of galaxies enables an increasingly thorough investigation of the imprints of the formation history in the outer, unrelaxed regions of galaxies, and a direct comparison to another tracer of galaxy formation, the internal kinematics.
Aims. Using the state-of-the-art hydrodynamical cosmological simulation *Magneticum Pathfinder*, we identify tidal tails, shells, streams, and satellite planes, and connect their existence to the amount of rotational support and the formation histories of the host galaxies.
Methods. Tidal features are visually classified from a three-dimensional rendering of the simulated galaxies by several scientists independently. Only features that were identified by at least half of the participating individuals are considered as existing features. The results are compared to observations of the MATLAS survey.
Results. Shells are preferentially found around kinematically slowly rotating galaxies in both simulations and observations, while streams can be found around all kind of galaxies with a slightly higher probability to be present around less rotationally supported galaxies. Tails and satellite planes, however, appear independently of the internal kinematics of the central galaxy, indicating that they are formed through processes that have not (yet) affected the internal kinematics.
Conclusions. As shells are formed through radial merger events while streams are remnants of circular merger infall, this suggests that the orbital angular momentum of the merger event could play a more crucial role in transforming the host galaxy than previously anticipated. The existence of a shell around a given slow rotator can further be used to distinguish the radial merger formation scenario from other formation pathways of slow rotators.

Key words. galaxies: evolution – galaxies: interactions – galaxies: kinematics and dynamics – galaxies: statistics – galaxies: structure

1. Introduction

The outer stellar regions of galaxies encode clues about their formation histories because of the larger relaxation times. Due to the low surface brightness (LSB) of these outskirts, deep imaging is necessary to detect faint structures created through tidal interactions and mergers with other galaxies, therefore storing information about the merger history (e.g., Johnston et al. 2008). These tidal features, such as shells, streams, or tidal tails, have recently been examined more closely through deep observations (e.g., Bílek et al. 2020) and high-resolution simulations (e.g., Karademir et al. 2019) with the aim of better understanding their connection with the merger histories of galaxies.

To study tidal features in a more statistically significant way, LSB features have been systematically classified in galaxy surveys, such as MATLAS (Duc et al. 2015; Bílek et al. 2020; Sola et al. 2022) or the Stellar Stream Legacy Survey (Martinez-Delgado et al. 2021). The features are oftentimes identified through visual inspection, though fully automated approaches have been developed as well. However, such automated methods can have issues with their sensitivity to LSB features (Sola et al. 2022).

Methods of identifying tidal features have also been applied to simulations. The possibility of tracing back individual galaxies and their tidal features through time enables a direct connection between the LSB structures with the formation histories of galaxies: shells typically form through mergers on radial orbits and streams through mergers on circular orbits (e.g., Amorisco 2015; Hendel & Johnston 2015; Pop et al. 2018; Karademir et al. 2019). Investigating the survival timescales in addition to the origin of different tidal features, Mancillas et al. (2019) found that shells and streams survive the longest and tails the shortest.

Satellite galaxies also reside in the outer galaxy regions and are expected to merge with the central galaxy in the future, potentially forming tidal features in the process. Already in 1976, Lynden-Bell found that the Magellanic Clouds and a number of globular clusters form a thin plane around the Milky Way, with more satellites identified to lie within it since then (e.g., Kroupa et al. 2005). Other well-known systems with satellite planes are the Andromeda Galaxy (e.g., Ibata et al. 2013) and Centaurus A (e.g., Müller et al. 2018). More recently, Heesters et al. (2021) found that roughly 25% of MATLAS galaxies feature a flattened satellite plane in their outskirts.

Satellite planes have been studied in cosmological simulations as well: some studies reported very few systems having such planes (e.g. Pawlowski et al. 2014), whereas others found better agreement with observations (e.g., Wang et al. 2013; Förster et al. 2022). Simulations further suggest that the arrangement of satellites is connected to the surrounding cosmic web (e.g., Welker et al. 2018), and some studies have concluded that thin planes of satellite galaxies are short-lived (Fernando et al. 2017). However,

it is still under debate how these satellite planes are connected to the central galaxy.

A direct imprint of a galaxy's formation history is also found in its kinematics. While late-type galaxies (LTGs) usually exhibit regular rotation patterns, early-type galaxies (ETGs) show a large variety of rotational properties. A kinematic classification of ETGs was introduced by Emsellem et al. (2007, 2011) for the SAURON and ATLAS^{3D} surveys, where ETGs are split into fast and slow rotators, depending on how rotationally supported they are. These rotation patterns are closely related to the formation of the galaxy, with slow rotators usually indicating a more violent accretion history (e.g., Schulze et al. 2018; Lagos et al. 2022).

As both the internal kinematics and the faint structures found in the outskirts of galaxies are remnants of their formation history, we investigate the correlation between these two tracers in simulations and observations in this work. We first introduce the simulations and observations in Section 2, followed by the details of our methods and the definition of the relevant properties in Section 3. Finally, the results are presented and discussed in Section 4, and are concluded in Section 5.

2. Simulations and Observations

2.1. The Magneticum Pathfinder Simulations

The galaxies classified in this work are extracted from the *Magneticum Pathfinder*[1] simulation suite (Dolag et al., in prep.), which consists of hydrodynamical cosmological simulations performed with GADGET-3, an extended version of GADGET-2 (Springel 2005). For details of the implementations, see Teklu et al. (2015). In particular, we use Box4 (uhr) (side length: 68 Mpc, with stellar particle mass $\langle m_* \rangle = 1.3 \times 10^6\,\mathrm{M}_\odot\,h^{-1}$ and softening length $\epsilon_* = 1$ kpc). Galaxies are identified using a modified version of SUBFIND adapted for baryonic matter (Springel et al. 2001; Dolag et al. 2009).

The galaxies from Magneticum Box4 (uhr) have been shown to agree well with observations, including their angular momenta (Teklu et al. 2015), kinematics (Schulze et al. 2018; van de Sande et al. 2019; Schulze et al. 2020), dynamics (Remus et al. 2017; Teklu et al. 2017; Harris et al. 2020), and their in-situ component fractions (Remus & Forbes 2022).

In this work, we include all main galaxies with virial masses $M_{\rm vir} \geq 7.1 \times 10^{11}\,\mathrm{M}_\odot$ and stellar masses $M_* \geq 2.4 \times 10^{10}\,\mathrm{M}_\odot$ to ensure sufficient resolution for identifying stellar tidal features. Additionally, we limit the sample to galaxies with stellar half-mass radii larger than 2 kpc, i.e., two times the stellar softening length (following Schulze et al. 2018). The resulting sample consists of 520 galaxies. Their ellipticities and λ_{R_e}-values (see Section 3.3) at one half-mass radius are taken from Schulze et al. (2018) and the satellite plane properties from Förster et al. (2022).

2.2. The MATLAS Sample

The observational comparison sample is taken from the MATLAS survey (Duc et al. 2015; Habas et al. 2020), which includes 177 massive ETGs with deep optical images. The MATLAS sample is part of the ATLAS^{3D} sample (Cappellari et al. 2011), which comprises 260 nearby galaxies (<42 Mpc) as a complete volume-limited sample. The MATLAS sample contains all ATLAS^{3D} galaxies that neither belong to the Virgo cluster nor are located near bright stars.

[1] www.magneticum.org

Specifically, we use the results obtained by Bílek et al. (2020) for the existence of tidal features around the 177 MATLAS galaxies, where tidal shells, streams, and tails were visually identified, and the identifications of satellite planes from Heesters et al. (2021). The ellipticities and λ_{R_e}-values at one effective radius are taken from Emsellem et al. (2011).

3. Methods & Definitions

For the comparison between the simulated and observed galaxies, in the following we introduce the different features and properties used in this work. These include the tidal features classified, the determination method of the satellite planes, and the distinction between fast and slow rotators.

3.1. Tidal Features: Shells, Streams, and Tidal Arms

The three types of tidal features considered are shells, streams, and tails. These indicate past or ongoing gravitational interactions with other galaxies. Shells appear as circular arcs centered around a galaxy (top panel of Figure 1). They have sharp outer borders and are believed to form through the radial infall and disruption of massive satellites (e.g., Quinn 1984; Pop et al. 2018; Karademir et al. 2019; Bílek et al. 2022). Streams are thin slivers of stars around the host galaxy (middle panel of Figure 1) that are formed through the tidal disruption of an infalling galaxy on a circular orbit (e.g., Karademir et al. 2019). Tails are stellar arms that come out from the host galaxy (bottom panel of Figure 1). These are the result of tidal interaction with another galaxy, where the interaction is either ongoing or occurred recently.

We classified the galaxies in Magneticum with respect to the existence of these tidal features by visual inspection of the three-dimensional stellar component, similar to the classification of Bílek et al. (2020) for the MATLAS sample. Seven scientists participated in the classification, where they were presented with a three-dimensional rendering of a given galaxy that was rotated to be viewed from all sides. The local environment around the individual galaxies was visible as well. The classification was performed independently by the participants, with each person stating whether they identified any tidal shells, streams, and tails, or not.

In the following, we consider a galaxy to have a given tidal feature if at least half of the participants were in favor of it. For the MATLAS classification by Bílek et al. (2020), this is considered to be the case if the classification score is at least 1 (the maximum score for them is 2, where 1 means the respective feature is likely to be present).

3.2. Satellite Planes

A galaxy is considered to have a satellite plane when at least 80% of its satellite galaxies build up a plane of thickness $\leq 0.2\,R_{\rm vir}$ and when the in-plane angular momentum makes up at least 90% of their total angular momentum. These properties are computed through the *momentum in thinnest plane* (MTP) method (Förster et al. 2022).

3.3. Fast and Slow Rotators

To distinguish fast from slowly rotating ETGs, we follow the approach taken by Emsellem et al. (2011). They determined an empirical cut in the λ_{R_e}-ϵ_e-plane, where λ_{R_e} is a 2D-projected proxy for the angular momentum within the effective radius, R_e,

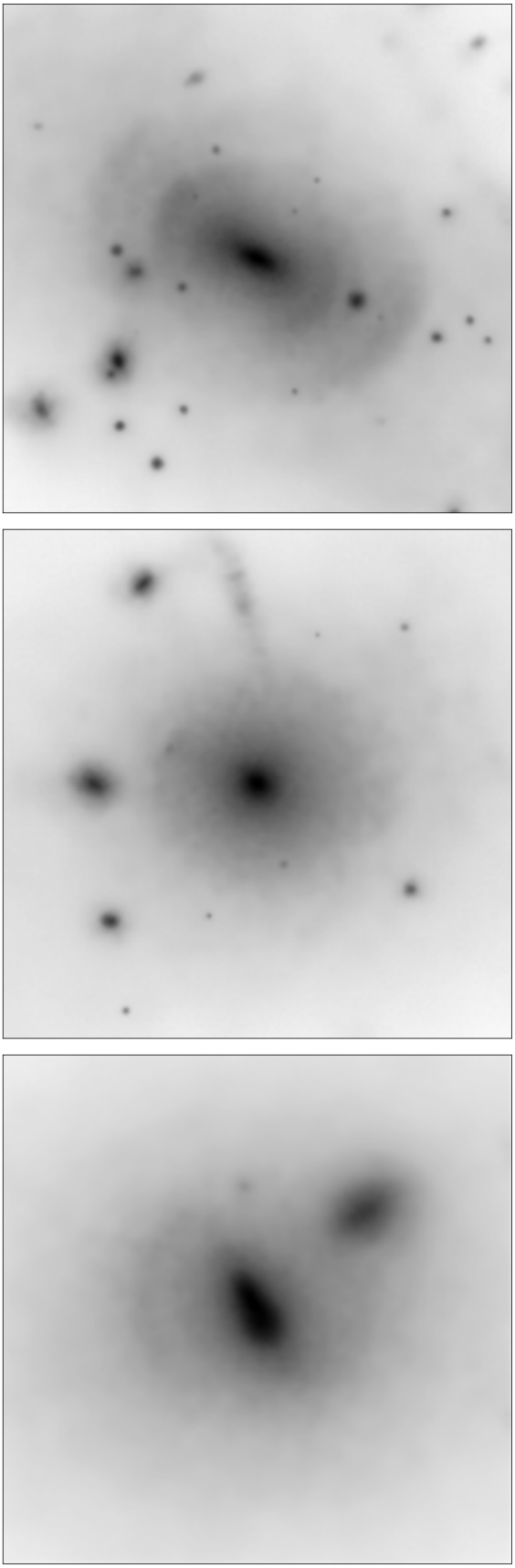

Fig. 1. Mock images of simulated galaxies from Magneticum Box4 (uhr) with prominent tidal features: shells (top), a stream (middle), and tails (bottom). The mock images were created with the software from Martin et al. 2022 for the r-band.

Table 1. Number and fraction of galaxies with stellar masses $M_* \geq 10^{11}$ $M_\odot$ having the respective tidal feature. The total number of galaxies analyzed in this mass range is 131.

Feature	Number	Fraction
Shells	14	11%
Streams	38	29%
Tails	16	12%

and ϵ_e is the ellipticity at the effective radius. The λ_{R_e}-value was introduced by Emsellem et al. (2007) as part of the SAURON project. Galaxies that fulfill $\lambda_{R_e} > 0.31\sqrt{\epsilon_e}$ are classified as fast rotators, all others as slow rotators.

We obtained these parameters for the simulated galaxies from Schulze et al. (2018) for the edge-on projections of the galaxies, since that maximizes the λ_{R_e}-values. The random projected values are also comparable to observations (Schulze et al. 2018). The main difference between calculating the parameters for simulations and observations is that for the former we use the stellar mass instead of the luminosity, assuming a constant mass-to-light ratio (see Schulze et al. 2018, for more details).

4. Results

4.1. Mass-Size Relation & Feature Statistics

Highlighting the galaxies with a given tidal feature in the mass-size relation shows that all three types of tidal features occur at all sizes and masses, with a clear preference for larger and more massive systems (first three panels of Figure 2). This preference is most likely due to the limited resolution of the simulation, with tidal features being better resolved for more massive systems. There is no visible correlation with the deviation from the average mass-size relation, however.

Considering only galaxies with stellar masses $M_* \geq 10^{11}$ $M_\odot$, about 10% to 20% have a given tidal feature (see Table 1). The occurrence of shells in 11% of the Magneticum galaxies agrees well with 12% from Atkinson et al. (2013), who used a different stellar mass range and somewhat different categories (see the discussion by Bílek et al. 2020), 17% from Bílek et al. (2020) for MATLAS (for the same stellar mass cut of 10^{11} $M_\odot$), and 18% from Pop et al. (2018) for the Illustris simulation. The fraction of galaxies having streams in Magneticum (29%) is very close to the 25% found for MATLAS. Finally, the fraction of galaxies having tails in Magneticum (12%) is larger than that in MATLAS (6%). Overall, the abundance of stellar tidal features found in the Magneticum Box4 simulation for the galaxies with larger stellar masses is consistent with previous findings.

We subdivided the galaxies from Magneticum into the morphological types using the classification from Teklu et al. (2017) based on the b-value (Teklu et al. 2015). The numbers of galaxies in each morphological class containing tidal features are listed in Table 2. While shells preferentially occur in ETGs, streams are found equally likely in all three types, and tails are more likely in intermediate galaxies and LTGs. A similar table for the kinematic classes is presented in Appendix B.

For the satellite planes, we find that only galaxies with stellar masses $\lesssim 10^{11}$ $M_\odot$ have thin planes of satellites around them. This is consistent with the results from Förster et al. (2022), who found that the more massive systems have thicker planes.

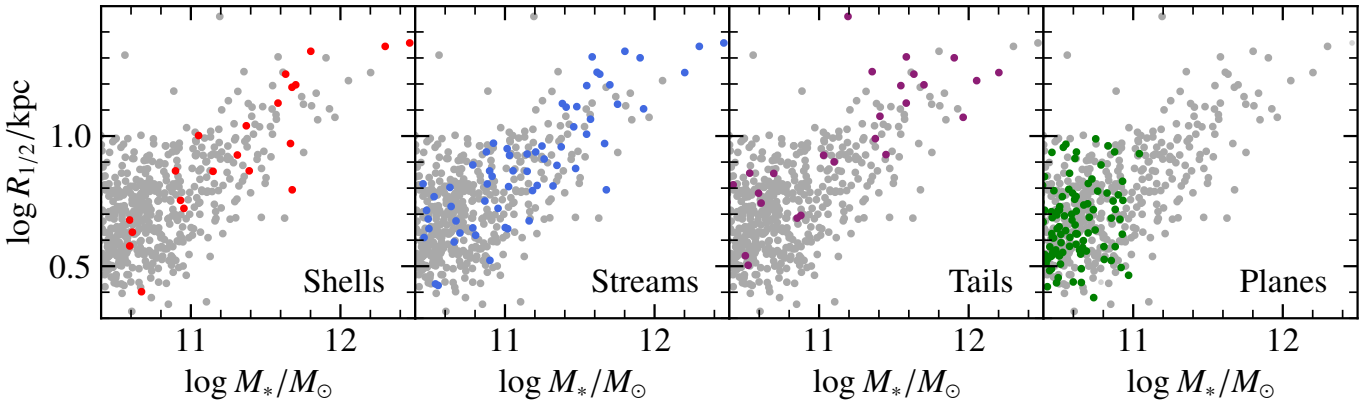

Fig. 2. Mass-size relation of the Magneticum galaxy sample with galaxies classified as having tidal features or satellite planes in color.

Table 2. Numbers and fractions of ETGs, intermediates, or LTGs having shells, streams, tails, or satellite planes for the full classified sample of 520 galaxies.

Type	All	Shells	Streams	Tails	Planes
ETGs	295	17 / 6%	37 / 13%	9 / 3%	49 / 17%
Interm.	172	4 / 2%	20 / 12%	12 / 7%	37 / 22%
LTGs	53	0 / 0%	5 / 9%	5 / 9%	14 / 26%

4.2. Tidal Features and Kinematics

We investigated the correlation between two known tracers of the accretion history of a galaxy, the appearance of tidal features and the internal galaxy kinematics. To measure the latter, we used the position of galaxies in the λ_{R_e}-ϵ_e-plane for both the observed and simulated galaxies (top and bottom of Figure 3, respectively). At first glance there are no clear differences between the distributions of galaxies with tidal features and the total sample for the observations and simulations. Only for the simulated galaxies the trend of shells being around slow rotators is visible. The galaxies with satellite planes are uniformly distributed and do not show any preference for slow or fast rotation, or for particularly round or elongated shapes (right panel of Figure 3).

The differences between the edge-on and random projection of galaxies in the λ_{R_e}-ϵ_e-plane are discussed by Schulze et al. (2018) in detail, especially with respect to the ellipticity, ϵ_e, clearly showing the problems when comparing ellipticities between simulations and observations. In contrast, λ_{R_e} is more directly comparable. Thus, we determined the cumulative histograms of λ_{R_e} for the total simulated and observed galaxy samples, and for the galaxies with the respective tidal features or satellite planes (Figure 4). Since the λ_{R_e}-distributions of the full samples are not identical (left-most panel), a direct comparison between the λ_{R_e}-distributions of galaxies having a certain tidal feature requires a correction to the values in the cumulative histograms. The method for this correction is described in Appendix A.

By adapting the simulated cumulative histograms to the observed parent distribution, the colored lines in Figure 4 are directly comparable with each other. Very similar distributions of λ_{R_e} are found for galaxies with a given tidal feature in the simulations and observations, clearly confirming that shells are mostly found around slow rotators. Streams have a slight preference for appearing around slow and intermediate rotators, which is more pronounced in the observations. Tidal tails are found around both slow and fast rotators with similar probabilities. However, there are differences for the presence of satellite planes: the simulations predict planes more commonly around fast rotators, while observations find a larger probability of planes around slow rotators, with Heesters et al. (2021) finding 40% around slow and 16% around fast rotators. This discrepancy may be related to the different methods of determining satellite planes. While the full 3D information from the simulation is incorporated to detect planes, the observations can only use information from the projected view. Therefore, the results on correlations between satellite planes and galaxy kinematics remain inconclusive.

The result that shells are more common around slow rotators suggests that there is a relation between the processes leading to low rotational support and the appearance of shells. Shells have been connected to massive mergers with radial infall (e.g., Amorisco 2015; Pop et al. 2018; Karademir et al. 2019), and slow rotators are found to often have formed through massive rapid merger events (e.g., Schulze et al. 2018; Lagos et al. 2022). Therefore, the existence of a shell is highly indicative of the observed slow rotator to have formed in a recent massive radial merger. This provides a way to distinguish this formation process from others like multiple small mergers (Naab et al. 2014) or internal feedback quenching (Lagos et al. 2022).

For confirmation, we traced back the most massive galaxy with shells in time, shown in Figure 5, with the orbit of the infalling galaxy that triggered the formation of the shells shown in red. For such massive galaxies, the best time and merger resolution can be expected given the storage limitations of cosmological simulations. In fact, the shells found around this galaxy were formed through a satellite with a mass ratio of 1:2.5 falling in radially at $z = 0.20$ (almost 2.5 Gyr ago), then falling back in again on the other side at $z = 0.13$ (1.7 Gyr ago). The back-and-forth movement led to the double shell structure found on two sides of the galaxy. This strongly supports the idea that shells form through mergers on radial orbits, albeit shown only for one example galaxy.

5. Conclusion

We classified galaxies from the Magneticum Box4 (uhr) simulation according to the existence of tidal features in their outskirts and compared these to the results from Bílek et al. (2020) for the MATLAS survey. The fraction of Magneticum galaxies having shells, streams, and tails are comparable to those found in observations and other simulations. We found a remarkable agreement with observations for the distribution of the kinematic parame-

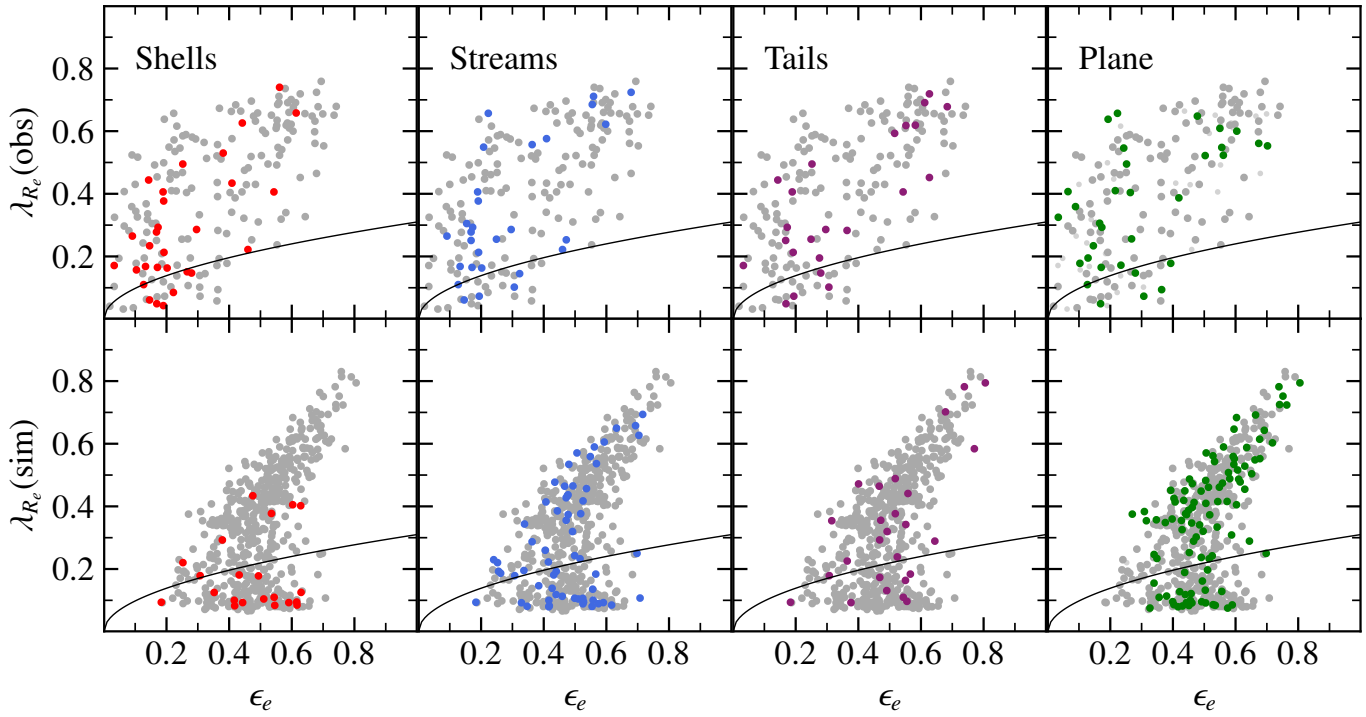

Fig. 3. Galaxies classified as having tidal features or a satellite plane in the λ_{R_e}-ϵ_e-plane in the MATLAS survey (*top row*) and in Magneticum Box4 (*bottom row*). Colored data points represent galaxies with the respective feature, large gray dots were classified as not having the respective feature, and small gray dots were not classified (only the case for the observed satellite planes). The values of λ_{R_e} and ϵ_e are determined at one effective radius for the observations and at one half-mass radius for the simulations. For the simulations, they are determined in the edge-on projection. The solid black lines indicate the border between fast and slow rotators (Emsellem et al. 2011), with fast rotators lying above the border. The measurements of shells, streams, and tails of MATLAS galaxies are from Bílek et al. (2020) and the measurements of the planes are from Heesters et al. (2021).

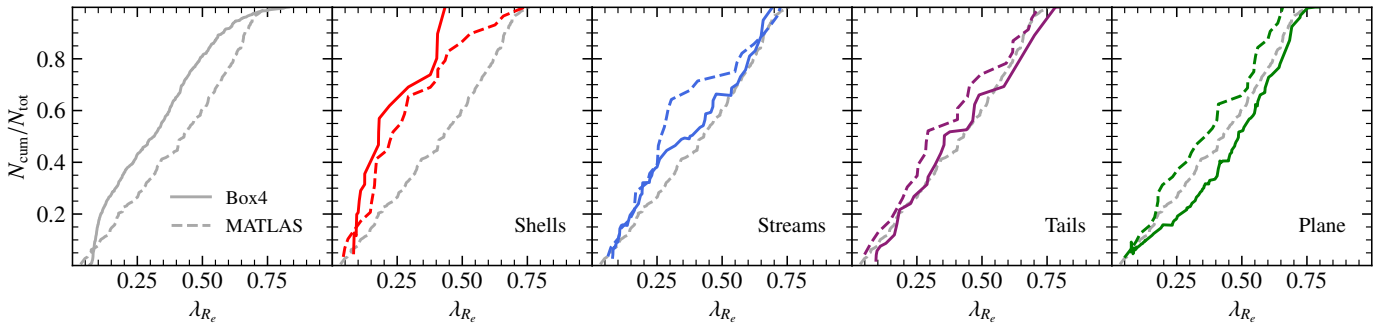

Fig. 4. Cumulative histograms of λ_{R_e} for the galaxies in the MATLAS survey (dashed lines) and in Magneticum Box4 (uhr) (solid lines). The first plot shows how the distributions between observations and simulations differ from each other. The cumulative histograms of the simulated galaxies in the other four panels are adapted to match the parent distribution of MATLAS to be directly comparable to the distributions of the MATLAS survey. Colored lines lying above the gray dashed line (the overall distribution of the MATLAS survey) indicate an increased presence of the respective tidal feature or satellite plane for slow rotators compared to fast rotators. The measurements of shells, streams, and tails of MATLAS galaxies are from Bílek et al. (2020) and the measurements of the planes are from Heesters et al. (2021).

ter λ_{R_e} for galaxies that have a given type of tidal feature. For both simulations and observations, slow rotators are the most likely to have shells, while streams preferentially occur around galaxies with low to medium rotational support. Tracing back a massive galaxy with multiple shells showed that these formed through an infalling satellite on a radial orbit. This supports the idea that shells are formed through massive radial merger events (e.g., Amorisco 2015; Karademir et al. 2019) that also transform the central galaxies into slow rotators, while more circular orbits of mergers do not necessarily lead to a full suppression of the rotational support. Moreover, the existence of shells around a slow rotator is highly indicative of a massive rapid radial merger event, providing the means to distinguish this formation scenario from others. Tails and satellite planes, on the other hand, occur independently of the morphology and internal kinematics of the central galaxy, which shows that these features are formed through processes that have not (yet) affected the internal kinematics.

Acknowledgements. We thank Pierre-Alain Duc and Elisabeth Sola for helpful discussions, and Nick Heesters for providing us with their data on the presence of satellite planes around MATLAS galaxies. We also thank Silvio Fortuné, Bendix Hagedorn, Elena Hernández Martínez, Tadziu Hoffmann, Lucas Kimmig

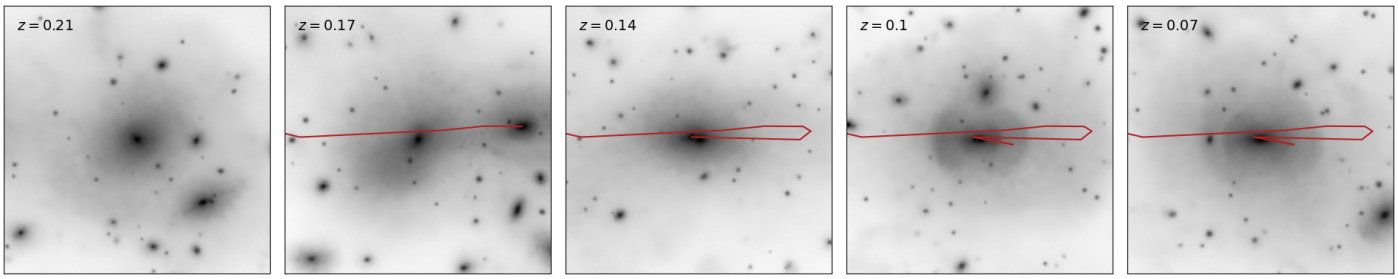

Fig. 5. Evolution of the first example galaxy from Figure 1. The shells develop after a massive radial merger event. The red lines trace the orbit of the infalling galaxy until the respective point in time.

for participating in the classification process of the galaxies in the simulation. LV acknowledges support by the COMPLEX project from the European Research Council (ERC) under the European Union's Horizon 2020 research and innovation program grant agreement ERC-2019-AdG 882679. The calculations for the hydrodynamical simulations were carried out at the Leibniz Supercomputer Center (LRZ) under the project pr83li (Magneticum). This research was supported by the Excellence Cluster ORIGINS, funded by the Deutsche Forschungsgemeinschaft under Germany's Excellence Strategy – EXC-2094-390783311. The following software was used for this work: Julia (Bezanson et al. 2017), Matplotlib (Hunter 2007).

References

Amorisco, N. C. 2015, MNRAS, 450, 575
Atkinson, A. M., Abraham, R. G., & Ferguson, A. M. N. 2013, ApJ, 765, 28
Bezanson, J., Edelman, A., Karpinski, S., & Shah, V. B. 2017, SIAM Review, 59, 65
Bílek, M., Duc, P.-A., Cuillandre, J.-C., et al. 2020, MNRAS, 498, 2138
Bílek, M., Fensch, J., Ebrová, I., et al. 2022, A&A, 660, A28
Cappellari, M., Emsellem, E., Krajnović, D., et al. 2011, MNRAS, 413, 813
Dolag, K., Borgani, S., Murante, G., & Springel, V. 2009, MNRAS, 399, 497
Duc, P.-A., Cuillandre, J.-C., Karabal, E., et al. 2015, MNRAS, 446, 120
Emsellem, E., Cappellari, M., Krajnović, D., et al. 2011, MNRAS, 414, 888
Emsellem, E., Cappellari, M., Krajnović, D., et al. 2007, MNRAS, 379, 401
Fernando, N., Arias, V., Guglielmo, M., et al. 2017, MNRAS, 465, 641
Förster, P. U., Remus, R.-S., Dolag, K., et al. 2022, arXiv e-prints, arXiv2208.05496
Habas, R., Marleau, F. R., Duc, P.-A., et al. 2020, MNRAS, 491, 1901
Harris, W. E., Remus, R.-S., Harris, G. L. H., & Babyk, I. V. 2020, ApJ, 905, 28
Heesters, N., Habas, R., Marleau, F. R., et al. 2021, A&A, 654, A161
Hendel, D. & Johnston, K. V. 2015, MNRAS, 454, 2472
Hunter, J. D. 2007, Computing in Science and Engineering, 9, 90
Ibata, R. A., Lewis, G. F., Conn, A. R., et al. 2013, Nature, 493, 62
Johnston, K. V., Bullock, J. S., Sharma, S., et al. 2008, ApJ, 689, 936
Karademir, G. S., Remus, R.-S., Burkert, A., et al. 2019, MNRAS, 487, 318
Kroupa, P., Theis, C., & Boily, C. M. 2005, A&A, 431, 517
Lagos, C. d. P., Emsellem, E., van de Sande, J., et al. 2022, MNRAS, 509, 4372
Lynden-Bell, D. 1976, MNRAS, 174, 695
Mancillas, B., Duc, P.-A., Combes, F., et al. 2019, A&A, 632, A122
Martin, G., Bazkiaei, A. E., Spavone, M., et al. 2022, MNRAS, 513, 1459
Martinez-Delgado, D., Cooper, A. P., Roman, J., et al. 2021, arXiv e-prints, arXiv2104.06071
Müller, O., Pawlowski, M. S., Jerjen, H., & Lelli, F. 2018, Science, 359, 534
Naab, T., Oser, L., Emsellem, E., et al. 2014, MNRAS, 444, 3357
Pawlowski, M. S., Famaey, B., Jerjen, H., et al. 2014, MNRAS, 442, 2362
Pop, A.-R., Pillepich, A., Amorisco, N. C., & Hernquist, L. 2018, MNRAS, 480, 1715
Quinn, P. J. 1984, ApJ, 279, 596
Remus, R.-S., Dolag, K., Naab, T., et al. 2017, MNRAS, 464, 3742
Remus, R.-S. & Forbes, D. A. 2022, ApJ, 935, 37
Schulze, F., Remus, R.-S., Dolag, K., et al. 2020, MNRAS, 493, 3778
Schulze, F., Remus, R.-S., Dolag, K., et al. 2018, MNRAS, 480, 4636
Sola, E., Duc, P.-A., Richards, F., et al. 2022, A&A, 662, A124
Springel, V. 2005, MNRAS, 364, 1105
Springel, V., White, S. D. M., Tormen, G., & Kauffmann, G. 2001, MNRAS, 328, 726
Teklu, A. F., Remus, R.-S., Dolag, K., et al. 2015, ApJ, 812, 29
Teklu, A. F., Remus, R.-S., Dolag, K., & Burkert, A. 2017, MNRAS, 472, 4769
van de Sande, J., Lagos, C. D. P., Welker, C., et al. 2019, MNRAS, 484, 869
Wang, J., Frenk, C. S., & Cooper, A. P. 2013, MNRAS, 429, 1502
Welker, C., Dubois, Y., Pichon, C., Devriendt, J., & Chisari, N. E. 2018, A&A, 613, A4

Table B.1. Numbers and fractions of galaxies with the given kinematic class having shells, streams, tails, or satellite planes for the subset of our full sample that was kinematically classified by Schulze et al. (2018). This subsample comprises 436 galaxies. The kinematic classes include regular rotators (RR), non-rotators (NR), galaxies with kinematically distinct cores (KDCs), and prolate rotators (PR).

Type	All	Shells	Streams	Tails	Planes
RR	286	2 / 1%	26 / 9%	8 / 3%	63 / 22%
NR	108	10 / 9%	16 / 15%	2 / 2%	19 / 18%
KDC	26	1 / 4%	6 / 23%	2 / 8%	1 / 4%
PR	16	3 / 19%	3 / 19%	2 / 13%	2 / 13%

Appendix A: Rescaling the Cumulative Distribution

The cumulative histogram of the simulated galaxies can be adapted to be directly comparable with that of the observations in the following way: For a given value of $\tilde{\lambda}_{R_e}$, the galaxies with values of $\lambda_{R_e} \leq \tilde{\lambda}_{R_e}$ can be determined for all the observed galaxies ($N_{\rm obs}(\leq\tilde{\lambda}_{R_e})$), all the simulated galaxies ($N_{\rm sim}(\leq\tilde{\lambda}_{R_e})$), and for the simulated galaxies with a given feature ($N_{\rm sim,feat}(\leq\tilde{\lambda}_{R_e})$). From these values, the cumulative number of simulated galaxies with a given feature adapted to the observational distribution of λ_{R_e} is

$$N_{\rm sim,feat,adap}(\leq\tilde{\lambda}_{R_e}) = N_{\rm obs}(\leq\tilde{\lambda}_{R_e}) \cdot \frac{N_{\rm sim,feat}(\leq\tilde{\lambda}_{R_e})}{N_{\rm sim}(\leq\tilde{\lambda}_{R_e})}. \quad \text{(A.1)}$$

Similarly, the adapted number of simulated galaxies with a given feature with values of $\lambda_{R_e} > \tilde{\lambda}_{R_e}$ can be determined:

$$N_{\rm sim,feat,adap}(>\tilde{\lambda}_{R_e}) = N_{\rm obs}(>\tilde{\lambda}_{R_e}) \cdot \frac{N_{\rm sim,feat}(>\tilde{\lambda}_{R_e})}{N_{\rm sim}(>\tilde{\lambda}_{R_e})}. \quad \text{(A.2)}$$

From these, the adapted normalized cumulative distribution (solid colored lines in Figure 4) is given by

$$\frac{N_{\rm cum}}{N_{\rm tot}} = \frac{N_{\rm sim,feat,adap}(\leq\tilde{\lambda}_{R_e})}{N_{\rm sim,feat,adap}(\leq\tilde{\lambda}_{R_e}) + N_{\rm sim,feat,adap}(>\tilde{\lambda}_{R_e})}. \quad \text{(A.3)}$$

Appendix B: Kinematic Classes

Table B.1 shows the numbers and fractions of galaxies with different kinematic classes (classified for Magneticum Box4 by Schulze et al. 2018) that have the respective tidal features or a satellite plane. For more information on the kinematic classes, see Schulze et al. (2018). In the table, we combined the distinct core (DC) and kinematically distinct core (KDC) classes into a single class of KDCs. The results for the KDCs and prolate rotators should be taken with caution because of the low number of galaxies with these kinematic features. Still, the clear trend emerges that regular rotators are much less likely to have any kind of tidal features, while especially non-rotators and prolate rotators have significantly higher fractions of shells. Interestingly, the KDCs are the least likely to have satellite planes, although this is based on only one galaxy out of 26. The fact that almost every fourth KDC has streams in its outskirts is consistent with many KDCs having decreasing λ_R-profiles, which generally have merger histories dominated by small mergers (Schulze et al. 2020). These could lead to tidal streams.